The interaction between AMPK beta 2 and the PP1-targeting subunit R6 is dynamically regulated by intracellular glycogen content

The interaction between AMPKβ2 and the PP1-targeting subunit R6 is dynamically regulated by intracellular glycogen content

Yvonne Oligschlaeger*, Marie Miglianico*, Vivian Dahlmans†, Carla Rubio-Villena‡, Dipanjan Chanda*, Maria Adelaida Garcia-Gimeno‡, Will A. Coumans*, Yilin Liu*, J. Willem Voncken†, Joost J.F.P. Luiken*, Jan F.C. Glatz*, Pascual Sanz‡ and Dietbert Neumann*[1]

*Department of Molecular Genetics, CARIM School for Cardiovascular Diseases, Maastricht University, 6200 MD Maastricht, The Netherlands
†Department of Molecular Genetics, GROW School for Oncology & Developmental Biology, Maastricht University, 6200 MD Maastricht, The Netherlands
‡Instituto de Biomedicina de Valencia, Consejo Superior de Investigaciones Cientificas (CSIC) and Centro de Investigación Biomédica en Red de Enfermedades Raras (CIBERER), 46010 Valencia, Spain

AMP-activated protein kinase (AMPK) is a metabolic stress-sensing kinase. We previously showed that glucose deprivation induces autophosphorylation of AMPKβ at Thr-148, which prevents the binding of AMPK to glycogen. Furthermore, in MIN6 cells, AMPKβ1 binds to R6 (PPP1R3D), a glycogen-targeting subunit of protein phosphatase type 1 (PP1), thereby regulating the glucose-induced inactivation of AMPK. In the present study, we further investigated the interaction of R6 with AMPKβ and the possible dependency on Thr-148 phosphorylation status. Yeast two-hybrid (Y2H) analyses and co-immunoprecipitation (IP) of the overexpressed proteins in human embryonic kidney (HEK) 293T) cells revealed that both AMPKβ1 and AMPK-β2 wild-type (WT) isoforms bind to R6. The AMPKβ–R6 interaction was stronger with the muscle-specific AMPKβ2-WT and required association with the substrate-binding motif of R6. When HEK293T cells or C2C12 myotubes were cultured in high-glucose medium, AMPKβ2-WT and R6 weakly interacted. In contrast, glycogen depletion significantly enhanced this protein interaction. Mutation of AMPKβ2 Thr-148 prevented the interaction with R6 irrespective of the intracellular glycogen content. Treatment with the AMPK activator oligomycin enhanced the AMPKβ2–R6 interaction in conjunction with increased Thr-148 phosphorylation in cells grown in low-glucose medium. These data are in accordance with R6 binding directly to AMPKβ2 when both proteins detach from the diminishing glycogen particle, which is simultaneous with increased AMPKβ2 Thr-148 autophosphorylation. Such a model points to a possible control of AMPK by PP1-R6 upon glycogen depletion in muscle.

Key words: AMP-activated protein kinase (AMPK), glycogen metabolism, glycogen targeting, phosphorylation, protein–protein interaction, R6.

INTRODUCTION

Muscular tissue, in particular skeletal muscle, is an important site for glucose storage. It has become evident that glucose disposal into glycogen is essential for co-ordinated glucose homoeostasis, as conditions limiting glycogen synthesis are associated with, for instance, hyperglycaemia and insulin resistance [1]. AMP-activated protein kinase (AMPK) is a metabolic energy sensor that mediates insulin-independent glucose transporter 4 (GLUT4) translocation to the plasma membrane resulting in increased glucose uptake [2]. Therefore, AMPK activation could normalize blood glucose levels in Type 2 diabetic patients. In response to various cellular stresses (e.g. contraction, nutrient deprivation), AMPK is activated and modulates downstream targets to induce catabolic ATP-producing processes and inhibit anabolic ATP-consuming processes, thereby restoring energy homoeostasis. AMPK consists of three subunits: the catalytic α subunit and two regulatory β and γ subunits; the latter are essential for regulating AMPK activity, as well as subcellular localization. AMPK subunits occur in different isoforms (α1 and α2; β1 and β2; γ1, γ2 and γ3) partly showing a tissue-specific expression pattern. Namely, β2 is the predominant isoform found in heart and skeletal muscle [3,4]. Accordingly, it has been reported that β1-knockout mice have a minimal phenotype in skeletal muscle [5], whereas β2-knockout mice have reduced skeletal muscle AMPK activity, exercise capacity and glucose uptake [6,7].

AMPK is known to shuttle between the nucleus [8,9] and the cytoplasm [10,11], suggesting that AMPK exerts compartment-specific effects in order to monitor and co-ordinate complex cell biological processes. The β subunit carbohydrate-binding module (CBM) allows AMPK to associate with glycogen [12,13], where it interacts with other glycogen-binding proteins including glycogen synthase (GS) [13] and glycogen phosphorylase (GP) [12]. Notably, β2 shows higher affinity for glycogen compared with β1 [14]. Acute 5-aminoimidazole-4-carboxamide ribonucleotide (AICAR)-induced AMPK activation inactivates GS via Ser-7 phosphorylation in skeletal muscle [15], although high levels of glucose 6 phosphate can override this inhibition [16].

The regulation of the activity status of localized AMPK is dependent on allosteric activation/repression and the action of upstream kinases capable of phosphorylating Thr-172 in the catalytic α subunit (e.g. LKB1, TAK1 and CaMKK2). Several protein phosphatases (e.g. PP1, PP2A and PP2C) dephosphorylate Thr-172, thus leading to AMPK inactivation. PP1 is an important

Abbreviations: AICAR, 5-aminoimidazole-4-carboxamide ribonucleotide; AMPK, AMP-activated protein kinase; CBM, carbohydrate-binding module; CIP, calf intestine phosphatase; DMEM, Dulbecco's modified Eagle's medium; EV, empty vector; G147R, Gly-147 residue for arginine; GM, growth medium; GP, glycogen phosphorylase; GS, glycogen synthase; HEK, human embryonic kidney; HRP, horseradish peroxidase; iFBS, heat-inactivated fetal bovine serum; IP, immunoprecipitation; ORF, open reading frame; PP1, protein phosphatase type 1; PPP1R3C, PTG/R5; R6, glycogen-targeting subunit PPP1R3D; Reg1, yeast-targeting subunit of PP1; Snf1, sucrose-non-fermenting 1; T148D, Thr-148 residue with aspartate; WT, wild-type; Y2H, yeast two-hybrid; β-CD, β-cyclodextrin.

[1] To whom correspondence should be addressed (email d.neumann@maastrichtuniversity.nl).

protein phosphatase in mammalian cells that is involved in proper co-ordination of glycogen metabolism by dephosphorylating target enzymes such as GS and GP. Recruitment of PP1 to its target substrates and to glycogen occurs by means of its glycogen-targeting proteins, such as PTG/R5 (PPP1R3C) [17] or R6 (PPP1R3D) [18,19]. Insight into PP1-mediated AMPK regulation came from our previous study [20], which showed that R6 physically interacts with the AMPKβ1 subunit, resulting in glucose-induced AMPK dephosphorylation by the PP1-R6 complex. Furthermore, we found that the CBM domain within the AMPKβ1 subunit is required for interaction with R6, as substitution of arginine for Gly-147 (G147R) resulted in total loss of AMPK–R6 interaction [20]. These results were consistent with parallel studies in yeast showing that sucrose-non-fermenting 1 (Snf1) is regulated by glucose, and that Gal-83 via its CBM interacts with yeast-targeting subunit of PP1 (Reg1), the orthologues of AMPKβ and R6, respectively [21], thus pointing to an evolutionarily conserved mechanism.

We recently reported that autophosphorylation of Thr-148 in the AMPKβ subunit interferes with the recruitment of AMPK to glycogen, suggesting that AMPK–glycogen localization is tightly regulated and linked to glycogen storage [22]. Given the direct binding of AMPKβ1 to R6 and the observed loss of this interaction using the AMPKβ1-G147R mutant, we hypothesized a role for AMPKβ Thr-148 phosphorylation. In the present study, we provide insight into the binding of AMPKβ2 to R6 in relation to glycogen content and AMPKβ2 Thr-148 phosphorylation. Our results indicate that the AMPKβ2–R6 interaction is dynamically controlled by glycogen content.

MATERIALS AND METHODS

Plasmids

For expression in mammalian cells, the cDNA of full-length AMPKβ1 and AMPKβ2 was amplified by PCR and ligated in-frame into the pmCherry expression vector (Clontech) via EcoRI and SalI restriction sites, as previously described [22]. An AMPKβ2–mCherry construct bearing a threonine-to-aspartate mutation on residue 148 (T148D) was generated using the Quik Change site-directed mutagenesis kit (Stratagene). The pcDNA3 constructs for expression of AMPKγ1 and myc–AMPKα1 were kindly provided by Dr D. Carling (Imperial College London, London, U.K.). The corresponding open reading frame (ORF) of AMPKβ2-T148D mutant was subcloned into pBTM116 to allow for expression in yeast (LexA-AMPKβ2-T148D). The pFLAG-R6 construct for mammalian expression of R6-wild type (WT) and R6 mutants (R6-RARA, -RAHA, -WDNAD and -WANNA) were generated as previously described, and pFLAG was used as empty vector (EV) control [20,23].

Other plasmids used for yeast two-hybrid (Y2H) analyses were pGADT7-Φ (GAD, empty plasmid), pGADT7-R6 (GAD-R6), pBTM-R6 (LexA-R6), pBTM-R6-RARA (LexA-R6-RARA), pBTM-R6-RAHA (LexA-R6-RAHA), pBTM-R6-WANNA (LexA-R6-WANNA), pBTM-R6-WDNAD (LexA-R6-WDNAD), pGADT7-AMPKβ1 (GAD-AMPKβ1), pGADT7-AMPKβ2 (GAD-AMPKβ2), pBTM-AMPKβ1 (LexA-AMPKβ1), pBTM-AMPKβ2 (LexA-AMPKβ2) [20, 23–25].

For retroviral overexpression and optimal detection of exogenous β2, full-length AMPKβ2-WT or AMPKβ2-T148D was amplified using PCR primers containing an optimized tetra-cysteine sequence (FlAsH-tag; FLNCCPGCCMEP). First, the corresponding ORF (FlAsH-tag) was subcloned into the SalI and NotI site of the mammalian β2-WT–mCherry or β2-T148D–mCherry construct, exchanging the mCherry tag for a FlAsH tag. Secondly, β2-WT–FlAsH or β2-T148D–FlAsH was amplified and subcloned into the EcoRI and SalI sites of the retroviral pBabe-puromycin backbone (kindly provided by Dr G. Nolan, Stanford University, CA, U.S.A.).

For retroviral overexpression of R6, the corresponding ORF (R6-WT) was amplified by PCR and subcloned into the BstXI and SalI restriction sites of the pBabe-puromycin retroviral backbone (kindly provided by Dr G. Nolan, Stanford University, CA, U.S.A.). The pBabe-puromycin EV was used as control. Primer sequences are available from D.N. upon request. All of the constructs were verified by DNA sequencing.

Cell culture

The human embryonic kidney (HEK) 293T cell line was cultured in Dulbecco's modified Eagle's medium (DMEM) with high glucose (25 mM) (Gibco), supplemented with 10 % (v/v) heat-inactivated fetal bovine serum (iFBS, Bodinco) and 1 % penicillin/streptomycin (Invitrogen), unless otherwise stated. For transient transfections, HEK293T cells were seeded to 30 % confluence in six-well plates (Greiner Bio-one) 24 h before transfection. For determination of protein–protein interactions, cells were co-transfected with AMPK (α1–myc, γ1 and β1-WT–mCherry or β2-WT/β2-T148D–mCherry), and/or FLAG–R6 (R6-WT/R6-RARA/R6-RAHA/R6-WANNA/R6-WDNAD) or FLAG EV plasmid DNA using Lipofectamine 2000 (Invitrogen) in antibiotic-free culture medium. At 6–8 h after transfection, transfection medium was replaced by normal growth medium (GM). At 48–72 h after transfection and continuous culturing (i.e. without change of medium), cells were harvested for glycogen or subjected to immunoprecipitation (IP) and Western blotting.

In order to induce glycogen depletion, HEK293T cells growing in high-glucose medium (DMEM with 25 mM glucose and 10 % iFBS), were subjected to forskolin treatment (100 μM, Sigma), low-glucose medium (DMEM with 3 mM glucose and 10 % iFBS) or glucose-deprived medium (DMEM and 10 % iFBS without glucose) for 16 h. To activate AMPK, cells were serum-starved in high- or low-glucose medium for 16 h, and subsequently treated with oligomycin (3 μM, Sigma) for 1 h.

The mouse skeletal muscle cell line C2C12 was kindly provided by Dr R.C. Langen (Maastricht University, Maastricht, The Netherlands). C2C12 cells were continuously cultured to approximately 80 % confluence in DMEM with high glucose (25 mM) (Gibco), supplemented with 10 % (v/v) iFBS and 1 % penicillin/streptomycin. For differentiation into myotubes, myocytes (75–85 % confluence) were further grown in differentiation medium (DMEM with 25 mM glucose (Gibco), supplemented with 2 % heat-inactivated horse serum (Invitrogen/Life Technologies) and 1 % penicillin/streptomycin (Invitrogen) for 4–5 days. Subsequently, cells were used in the corresponding experiments. In order to induce glycogen depletion, myotubes were maintained in low-glucose medium (DMEM with 3 mM glucose, supplemented with 2 % iFBS), for 16 h. In order to activate AMPK, myotubes were maintained in high or low glucose for 16 h as described above, and subsequently treated with oligomycin (5 μM) for 30 min.

Retroviral infections

In order to study protein–protein interactions in C2C12 myotubes, growing cells were infected with FlAsH-tagged AMPKβ2-WT or -T148D, or FLAG-tagged R6 retrovirus. Briefly, retroviral systems and Phoenix helper-free retrovirus producer cell lines

were used as described previously [26–28]. Amphotropic retroviral supernatants were produced as previously described [22]. Briefly, 24–48 h after calcium phosphate/DNA transfection of producer cells, supernatants were harvested, filtered (0.45 μm filters; Corning) and used for infection of C2C12 cells in the presence of 4 μg/ml polybrene (Sigma). For infections, cells were incubated with virus particles for 6–8 h and then allowed to recover for 48 h on fresh medium, before selection pressure was applied. Stably infected cells were selected 2 days post-infection with 4 μg/ml puromycin for 36–48 h preceding experiments.

Immunoprecipitation and Western blotting

IP procedures were performed as previously described [22]. Briefly, exogenous myc–AMPKα1 was immunoprecipitated using anti-myc-tag antibody (9B11, Cell Signaling Technology), exogenous R6 was immunoprecipitated using anti-FLAG-tag antibody (F3165, Sigma) and endogenous AMPK was immunoprecipitated using a combination of anti-AMPKα1 and anti-AMPKα2 antibodies raised in sheep (kindly provided by Dr D.G. Hardie, University of Dundee, Dundee, UK), followed by incubation with Protein G–Sepharose beads (GE Healthcare). Western blot analysis was carried out using primary antibodies against the following: myc-tag, total AMPKα, AMPKβ1, AMPKβ2, phospho-AMPK-Thr-172 (all from Cell Signaling Technology), FLAG-tag (F3165, Sigma), and phospho-AMPKβ2-Thr-148 [22]. Detection was performed according to its primary antibody using anti-rabbit (Cell Signaling Technology) and anti-mouse (Dako) horse radish peroxidase (HRP)-conjugated secondary antibodies, followed by chemiluminescence.

In order to investigate the role of glycogen, myc–AMPKα1 was immunoprecipitated using the anti-myc-tag antibody after the addition of the glycogen mimic β-cyclodextrin (β-CD; 5 mM, Sigma) for 1 h at 4 °C. Subsequently, immune complexes were electrophoresed by SDS/PAGE and analysed by Western blot analysis, as described above.

Biochemical intracellular glycogen measurement

Intracellular glycogen content was measured, as previously described [22]. Briefly, HEK293T cells (non-transfected or transfected) or stably infected C2C12 myotubes were lysed in potassium hydroxide (30 %) and boiled at 70 °C for 30 min. Subsequently, samples were cooled to 25 °C before sodium sulfate (6 %, w/v) and ethanol (99.5 %, v/v) were added at a 1:1:3 ratio. After thorough mixing, samples were rotated top-over-top at 4 °C for 30–60 min. The precipitate was collected by centrifugation at 2300 ***g*** (Eppendorf Centrifuge 5415 R) for 5 min at 4 °C. To hydrolyse glycogen, pellets were dissolved in 1 M HCl and boiled at 100 °C for 2 h. Samples were cooled before neutralization using 2 M sodium hydroxide. Hydrolysates were used for glucose determination using a glucose assay kit (Sigma), according to the manufacturer's instructions.

Determination of glucose uptake

The glucose uptake protocol was adapted from earlier work [29]. Briefly, stably infected C2C12 myotubes were incubated with the uptake buffer containing deoxy-D-glucose (4 μM), with tracer amounts of ^{3}H-labelled 2-deoxy-D-glucose, for 10 min. Surplus substrate was removed by washing the cells with ice-cold uptake buffer and cells were lysed in 0.1 M sodium hydroxide. Incorporated glucose was assessed by scintillation counting of ^{3}H in lysates.

Preparation of skeletal muscle tissue homogenates

Gastrocnemius muscle was taken from one female WT C57/BL6 mouse of the regular Maastricht University breeding programme, which was approved by the Animal Ethics Committee of Maastricht University and performed according to the Dutch regulations. After killing, tissues were freeze clamped between aluminium tongs pre-cooled in liquid nitrogen and stored at − 80 °C until analysis. Muscle extract was prepared essentially as previously described [30]. Briefly, the tissue sample was extracted in SET buffer (250 mM sucrose, 2 mM EDTA and 10 mM Tris/HCl pH 7.4) in the presence of protease and phosphatase inhibitors (Complete and PhosStop; Roche) by homogenization and ultrasound treatment, followed by centrifugation. Supernatant was used for IP (see above) using the indicated antibodies.

Yeast two-hybrid analyses

Y2H analysis was performed as previously described [20,24]. Briefly, interaction analysis using yeast THY-AP4 strain (*MATa, ura3, leu2, lexA::lacZ::trp1, lexA::HIS3, lexA::ADE2*) co-transformed with the indicated combination of plasmids (see above). Transformants were grown in selective 4 % glucose synthetic complete medium lacking the corresponding supplements to maintain selection for plasmids. The strength of the interaction was determined by measuring β-galactosidase activity in permeabilized yeast cells and expressed in Miller units. In all Y2H analyses, similar protein levels were obtained from the expression constructs, as verified in the crude extracts from the different yeast transformants.

Statistical analysis

All plotted data are presented as means $\pm$ S.E.M., unless otherwise stated. Statistical differences were evaluated using unpaired Student's *t* test and statistical analysis software Prism 4 (GraphPad Software). P values equal to or less than 0.05 were considered statistically significant.

RESULTS

R6 preferentially interacts with AMPKβ2

We previously demonstrated that R6 (PPP1R3D), one of the glycogen-targeting subunits of PP1, physically interacts with AMPKβ1 in MIN6 pancreatic β cells [20]. To verify AMPKβ1–R6 interaction in HEK293T cells, we overexpressed myc-tagged AMPK heterotrimers (myc–α1, β1–mCherry, γ1), together with FLAG-tagged R6 (FLAG–R6) or EV control. Physical interaction between AMPKβ1 and R6 was assessed by IP of AMPK from cells that were routinely cultured under glucose-rich conditions (25 mM glucose) (Figure 1A). Pull-down of myc–AMPKα1 resulted in co-IP of both mCherry-tagged AMPKβ1 (65 kDa) and FLAG-tagged R6, indicating formation of the heterotrimeric AMPK complex and the interaction with R6 (Figure 1A). As expected, FLAG–R6 signal was absent from cells transfected with EV. Next, we investigated the interaction between muscle-specific AMPKβ2 heterotrimers (myc–α1, β2–mCherry, γ1) and R6 (FLAG–R6) using co-transfection and IP in HEK293T cells. As both proteins co-immunoprecipitated, this data points to the occurrence of a physical interaction between R6 and AMPKβ2 (Figure 1B). Interestingly, co-IP appeared stronger in the presence of AMPKβ2 compared with β1. These data were further confirmed by Y2H analyses: in Figure 1C it is shown that R6 binds to both AMPKβ1 and AMPKβ2, whereas the interaction

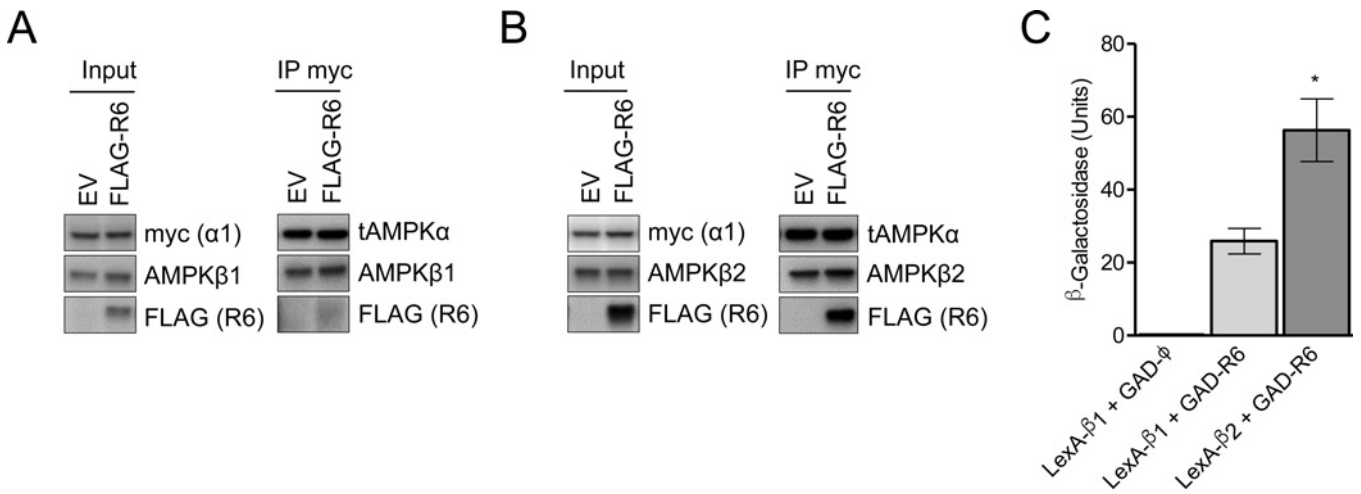

Figure 1 R6 preferentially interacts with AMPKβ2

(**A** and **B**) HEK293T cells transiently overexpressing FLAG–R6 and heterotrimers of AMPKβ1 (myc–α1, γ1, AMPKβ1–mCherry) (**A**) or AMPKβ2 (myc–α1, γ1, AMPKβ2–mCherry) (**B**). FLAG EV was used as control. Cells were continuously cultured under high-glucose (25 mM) conditions and harvested 56 h post-transfection. Interaction between AMPKβ1/AMPKβ2 and R6 was assessed by immunoprecipitating the heterotrimeric AMPK complex from 800 μg of lysate using the anti-myc-tag antibody. Western blots were assessed using the indicated antibodies. Representative Western blots are shown. (**C**) Yeast THY-AP4 strain (see the Materials and methods section) was transformed with the indicated combination of plasmids. Transformants were grown in high-glucose (4% glucose) medium and protein interactions were estimated by measuring the β-galactosidase activity. EV pGADT7 (GAD-Φ) served as control. Values correspond to means from at least six different transformants (bars indicate S.D.). $^*P < 0.001$ compared with LexA-AMPKβ1-WT + GAD-R6.

between AMPKβ2 and R6 is significantly stronger than the one between AMPKβ1 and R6. Combined, these findings suggest that R6 prefers interaction with AMPKβ2 over AMPKβ1.

R6 interaction with AMPKβ2 requires its substrate-binding motif

Recently, a number of functionally distinct protein domains have been identified in the R6 glycogen-targeting subunit of PP1 [23]. R6 is composed of domains that mediate binding to carbohydrates (via its CBM), binding to the PP1 catalytic subunit (PP1c; RVXF motif), and to the glycogen metabolism-related substrates of PP1 (via the highly conserved WDNND motif). To investigate whether and which of these motifs are involved in the interaction between the AMPKβ subunit and R6, we performed studies in HEK293T cells co-expressing AMPKβ2 complex (myc–α1, β2–mCherry, γ1) with FLAG–R6, the latter carrying various mutations corresponding to its protein motifs [23] (Figures 2A and 2B). We again immunoprecipitated myc–AMPKα1 using a myc-directed antibody. Of note, endogenous R6 was not detected either in lysate or in immunoprecipitated material, thereby substantiating the need for FLAG–R6 overexpression to study the interaction between AMPKβ2 and R6 (Figure 2B: EV condition). R6 carried various domain-specific mutations: in both R6-RARA and R6-RAHA mutants, the hydrophobic valine and phenylalanine residues within putative R6-RVXF motifs were replaced by alanine, allowing us to probe the role of the PP1-binding motif in AMPKβ2–R6 binding (Figure 2B). R6-RARA, a mutant known to have lost its capacity to bind to endogenous PP1c but not to PP1 substrates [23], presented a similar AMPKβ2-binding profile compared with WT, non-mutated R6 (R6-WT; Figure 2B, right panel). The R6-RAHA mutant that carried mutations in a domain close to the substrate-binding motif, however, had completely lost its ability to interact with AMPK (Figure 2B, right panel). These data were reproduced in a reciprocal Y2H assay using AMPKβ2 as bait (Figure 2C). Furthermore, the substrate-binding motif (WDNND) was mutated to study its effect on AMPKβ2–R6 interaction. In one of the mutants, the two aspartate residues present within the WDNND motif were replaced by alanine (R6-WANNA mutant), whereas in the R6-WDNAD mutant the second asparagine residue was replaced by alanine. Whereas the R6-WDNAD mutant was still capable of interacting with AMPKβ2, the WANNA mutation abolished AMPKβ2 binding (Figures 2B, right panel, and 2C). In good agreement, Y2H analyses using AMPKβ1 or AMPKβ2 as bait confirmed that the binding of R6 to the AMPKβ subunits depended on the R6 substrate-binding motif being intact (Figures 2C and 2D). Thus, we show that the AMPKβ–R6 interaction requires the R6 substrate-binding motif. In all subsequent experiments, we concentrated on the AMPKβ2–R6 interaction.

AMPKβ2 Thr-148 mutant shows reduced interaction with R6

Previously, we showed that substitution of arginine for the Gly-147 residue (G147R) within the β1-CBM domain abolished the interaction of AMPK with R6 [20], indicating that AMPKβ1 requires the CBM for interaction with R6. More recently, we demonstrated that autophosphorylation at the β Thr-148 residue, centrally located in the CBM, prevents AMPK from binding to carbohydrates such as glycogen [22]. As we show here that R6 also interacts with AMPKβ2, we next investigated whether Thr-148 is required for the AMPKβ2–R6 interaction. To this end, a phospho-mimicking AMPKβ2 mutant was generated by replacing the Thr-148 residue with aspartate (T148D) within the β2-CBM. Transiently transfected HEK293T cells co-expressing FLAG–R6 and AMPK heterotrimers (myc–α1 and γ1 in combination with either β2-WT– or β2-T148D–mCherry) were cultured under high-glucose conditions (25 mM) and used for co-IP analysis. Impaired interaction between AMPKβ2 and R6 was observed in cells overexpressing mutant AMPKβ2-T148D (Figure 3A, right panel); relevantly, FLAG–R6 and β2–mCherry were expressed at comparable levels (Figure 3A, left panel). Independent Y2H analyses corroborated these findings: the T148D mutation decreased the interaction between AMPKβ2 and R6 (Figure 3B). Taken together, our data indicate that Thr-148 mutation into aspartate results in loss of the AMPKβ2–R6

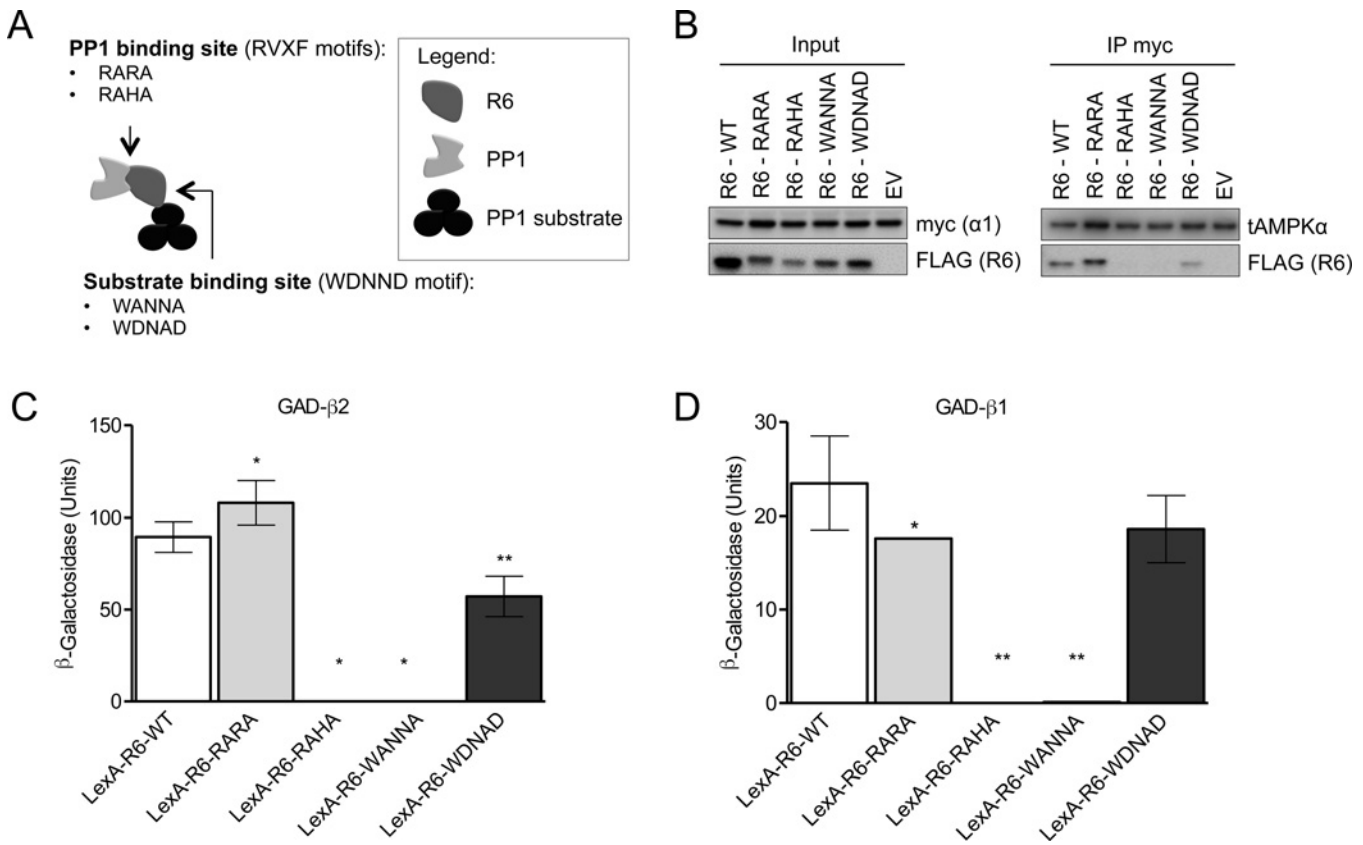

Figure 2 R6 interaction with AMPKβ2 requires its substrate-binding motif

(**A**) Schematic model indicating the PP1- and substrate-binding sites of R6, and its corresponding mutations. (**B**) HEK293T cells transiently co-expressing AMPKβ2 heterotrimers (myc–α1, γ1, AMPKβ2–mCherry) and FLAG–R6-WT (R6-WT) or mutant (R6-RARA, R6-RAHA, R6-WANNA, R6-WDNAD respectively) were continuously cultured under high-glucose (25 mM) conditions and harvested 48 h post-transfection. FLAG EV was used as control. Interaction between AMPKβ2 and R6 was assessed by immunoprecipitating the heterotrimeric AMPK complex from 450 μg of lysate using the anti-myc-tag antibody. Western blots were assessed using the indicated antibodies. Representative Western blots are shown. (**C** and **D**) Yeast THY-AP4 strain (see the Materials and methods section) was transformed with GAD-AMPKβ2 (**C**) or GAD-AMPKβ1 (**D**) plasmids and LexA-R6 plasmids as indicated. Transformants were grown in high-glucose (4 % glucose) medium and protein interactions were estimated by measuring the β-galactosidase activity. Values correspond to means from at least six different transformants (bars indicate S.D.). $^{*}P < 0.05$ and $^{**}P < 0.001$ compared with LexA-R6-WT.

interaction, suggesting that an intact Thr-148 residue is essential for the formation of the AMPKβ2–R6 complex under glucose-rich culturing conditions.

Glycogen depletion enhances the interaction between AMPKβ2 and R6

To investigate whether the interaction between AMPKβ2 and R6 is responsive to variation in glycogen level, we aimed to deplete cellular glycogen content. Hence, HEK293T cells were either pharmacologically treated with forskolin, a compound inducing glycogen breakdown [31], or glucose-deprived, after which glycogen content was assessed. Because R6 is known to have glycogenic properties [24], we included non-transfected control cells and compared these with cells that were either transfected with FLAG–R6 alone or co-transfected with all three subunits of AMPK (myc–α1, β2-WT–mCherry, γ1). As expected, cells overexpressing FLAG–R6 showed high glycogen content (both in the absence and presence of overexpressed AMPKβ2 complex): basal glycogen levels were 30–40-fold increased compared with non-transfected control cells (Figure 4A). Both forskolin treatment and glucose deprivation significantly lowered the intracellular glycogen levels in all cell lines, as compared with their respective controls (Figure 4A). To assess the effect of cellular glycogen content on AMPKβ2–R6 interaction, HEK293T cells overexpressing both FLAG–R6 and AMPKβ2 heterotrimers were either treated with forskolin or glucose-deprived for 16 h. Reduction of cellular glycogen content, either by forskolin treatment or by glucose deprivation, substantially enhanced the interaction between AMPK and R6 that was accompanied by a similar increase in the Thr-172 phosphorylation level (Figure 4B, right panel); as total levels of AMPK and R6 did not change within the experimental time frame (Figure 4B, left panel), this ruled out any possible interference by altered expression. Furthermore, we examined whether the binding of overexpressed AMPKβ2 to FLAG–R6 is reversible (Figure 4C). Expectedly, immunoprecipitates of AMPK from cells that were cultured in low-glucose (3 mM) medium displayed clear interaction with R6. When cells were switched back to incubation in high-glucose (25 mM) medium, this association decreased time-dependently, resulting in a complete loss of the AMPKβ2–R6 interaction after 30 min. Collectively, our data suggest that the interaction between AMPKβ2 heterotrimers and R6 is dynamic and inversely correlated with cellular glycogen level.

To independently examine a possible direct effect of glycogen on the AMPKβ2–R6 binding, we next used β-CD, a model sugar that mimics glycogen, in competitive binding IP experiments in

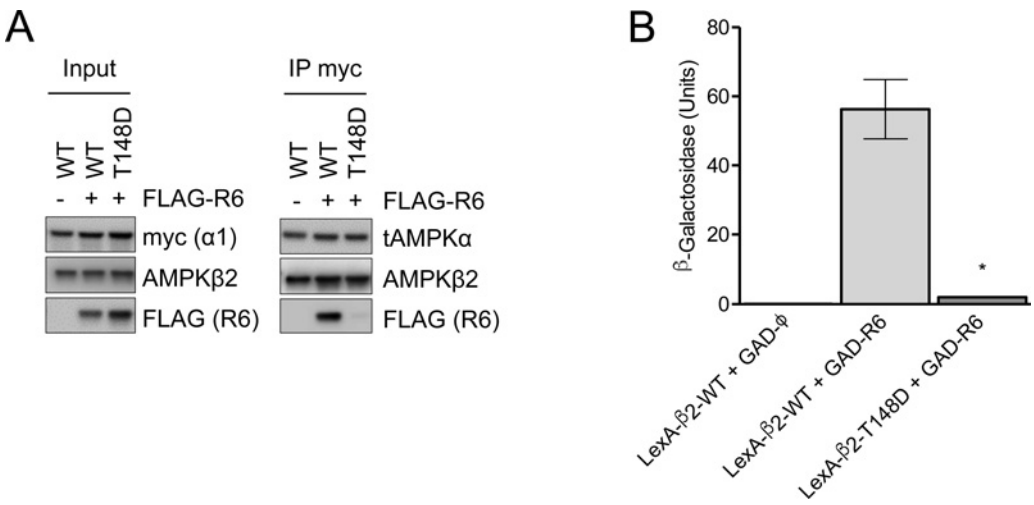

Figure 3 AMPKβ2 Thr-148 mutant shows reduced interaction with R6

(**A**) HEK293T cells transiently transfected with myc–α1, γ1 and mCherry-tagged AMPKβ2 WT or Thr-148 mutant (T148D) were co-transfected either with FLAG–R6 (+), or FLAG EV (−) as control. Cells were cultured under high-glucose (25 mM) conditions, and harvested 56 h post-transfection. Interaction between AMPKβ2 and R6 was assessed by immunoprecipitating the heterotrimeric AMPK complex from 800 μg of lysate using the anti-myc-tag antibody. Western blots were assessed using the indicated antibodies. Representative Western blots are shown. (**B**) Yeast THY-AP4 strain was transformed with plasmids LexA-AMPKβ2-WT or LexA-AMPKβ2-T148D and GAD-R6 as indicated. Transformants were grown in high-glucose (4% glucose) medium and protein interactions were estimated by measuring the β-galactosidase activity. EV pGADT7 (GAD-Φ) served as control. Values correspond to means from at least six different transformants (bars indicate S.D.). *$P < 0.001$ compared with LexA-AMPKβ2-WT + GAD-R6.

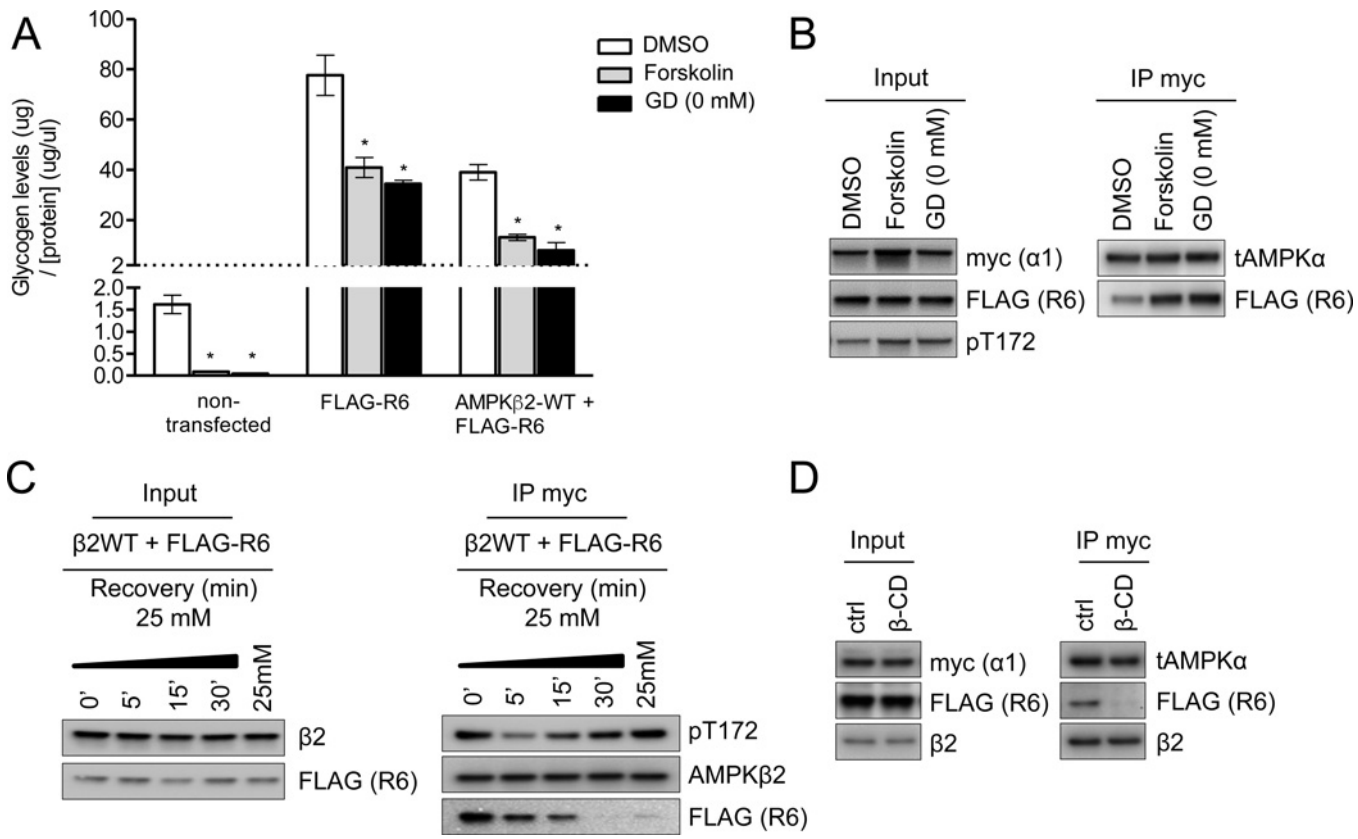

Figure 4 Glycogen depletion enhances the interaction between AMPKβ2 and R6

(**A** and **B**) HEK293T cells non-transfected, transiently transfected with FLAG–R6 alone or co-transfected with FLAG–R6, myc–α1, γ1 and mCherry-tagged AMPKβ2-WT were cultured under high-glucose (25 mM) conditions. Prior to lysis, cells were treated with forskolin (100 μM) or DMSO (control) under high-glucose conditions or cells were glucose-deprived (GD, 0 mM) for 16 h. (**A**) Intracellular glycogen level was determined as described in the Materials and methods section. Levels were corrected for corresponding protein concentrations. *$P < 0.05$ compared with corresponding DMSO controls; $n = 2$. (**B**) Heterotrimeric AMPK was immunoprecipitated from 500 μg of lysate using the anti-myc-tag antibody, followed by Western blot analysis using the indicated antibodies. (**C**) HEK293T cells transiently transfected with FLAG–R6, myc–α1, γ1 and mCherry-tagged AMPKβ2-WT were cultured under low-glucose (3 mM) conditions and recovered with high-glucose medium (25 mM) for the indicated time period before lysis and immunoprecipitation. (**D**) HEK293T cells were transiently co-transfected as indicated and harvested 56 h post-transfection. Cells were continuously grown under high-glucose (25 mM) conditions. β-CD (5 mM) was added prior to IP. Representative Western blots are shown.

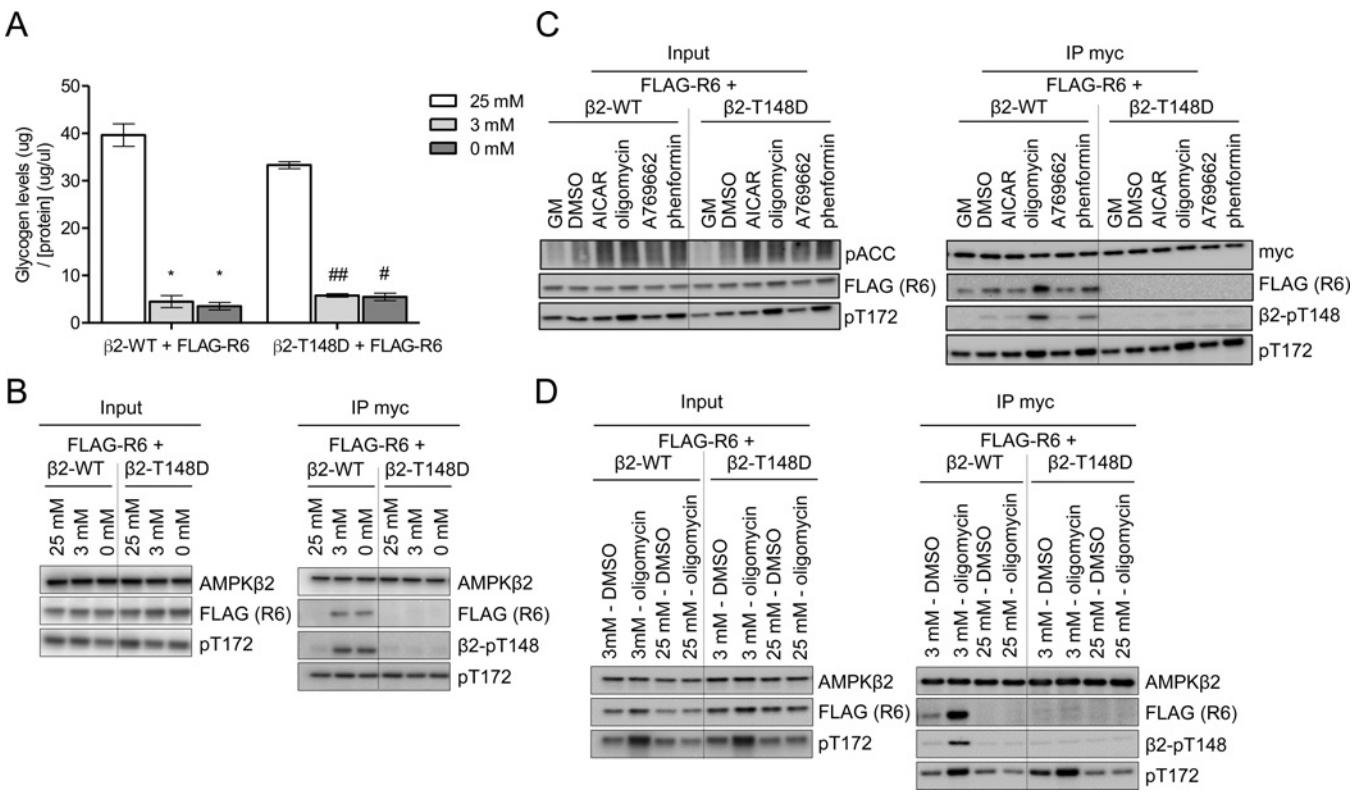

Figure 5 AMPKβ2–R6 interaction is enhanced in conjunction with increased AMPKβ2 Thr-148 phosphorylation

HEK293T cells were transiently transfected for co-expression of AMPKβ2 heterotrimers (myc–α1, γ1, mCherry-tagged AMPKβ2-WT or -T148D) and FLAG–R6. (**A** and **B**) Prior to lysis, cells were cultured under various glucose conditions (i.e. 25, 3 or 0 mM) for 16 h. (**A**) Intracellular glycogen levels were biochemically determined and corrected for the corresponding protein concentrations. $^{*}P < 0.01$ compared with WT 25 mM, $^{\#}P < 0.01$ compared with T148D with 25 mM glucose, $n = 2$. (**B**) Heterotrimeric AMPK was immunoprecipitated from 350 μg of lysate using the anti-myc-tag antibody, followed by Western blot analysis using the indicated antibodies. (**C**) Cells were either maintained in GM (25 mM glucose + 10% iFBS), or serum-starved (5.5 mM glucose) for 16 h and subsequently treated with DMSO (control) or a variety of AMPK activators for 1 h, as indicated. AMPK complexes were immunoprecipitated from 350 μg of lysate using the anti-myc-tag antibody, followed by Western blot analysis using various antibodies. (**D**) Cells were serum-starved both under low-(3 mM) and high-(25 mM) glucose conditions for 16 h, prior to 1 h treatment with oligomycin (3 μM) or DMSO (control). AMPK was immunoprecipitated from 500 μg of lysate as described in (**B**), followed by Western blot analysis using the indicated antibodies. Representative Western blots are shown.

HEK293T cells cultured under high glucose. Addition of β-CD completely disrupted the interaction between AMPKβ2 and R6 (Figure 4D, right panel). Combined, these data suggest that, under glucose-rich conditions, glycogen disturbs the AMPKβ2–R6 interaction, indicating that glycogen interferes with and therefore weakens the interaction between AMPKβ2 and R6.

AMPKβ2–R6 interaction is enhanced by glycogen depletion in conjunction with increased AMPKβ2 Thr-148 phosphorylation

Next, we assessed the impact of Thr-148 phosphorylation on the glycogen-modulated AMPKβ2–R6 interaction. To this end, we co-transfected HEK293T cells with AMPK heterotrimers (myc–α1, γ1 and either mCherry-tagged β2-WT or -T148D mutant) and FLAG–R6, and challenged the cells for 16 h with various concentrations of glucose. The expression of AMPKβ2-T148D mutant did not affect the glycogenic activity of FLAG–R6 in cells cultured under high-glucose conditions (Figure 5A), indicating that glycogen production depends on the function of R6 but not on the interaction between R6 and AMPKβ2. Reduced availability of glucose (i.e. 3 or 0 mM) correlated with significantly decreased intracellular levels of glycogen in both AMPKβ2-WT- and -T148D-expressing cells (Figure 5A). Interestingly, we observed increased levels of Thr-148 phosphorylation in β2-WT immunoprecipitates upon lowering glucose conditions, although we did not find changes in the levels of AMPK Thr-172 phosphorylation, either in cellular lysates or in the precipitates from β2-WT- or β2-T148D-expressing cells (Figure 5B). Low glycogen content enhanced AMPKβ2–R6 interaction (Figure 5B; cf. Figure 4). Whereas AMPKβ2-WT–R6 binding was readily detectable, T148D mutation completely abolished AMPKβ2 interaction with R6, independent of the glycogen status (Figure 5B; cf. Figure 3). Furthermore, we investigated the effect of AMPK activation on the AMPKβ2–R6 interaction using various AMPK-activating stimuli (Figure 5C). Again, the AMPKβ2-T148D mutant did not associate with R6 under any of the conditions tested. AMPK activation generally enhanced the AMPKβ2-WT–R6 interaction. Oligomycin exhibited the strongest AMPK-activating effect (Thr-172 phosphorylation in Figure 5C, left panel). AMPKβ2 Thr-148 phosphorylation and the binding of R6 to AMPKβ2 were greatly enhanced by oligomycin (Figure 5C, right panel). Next, we exposed cells to oligomycin in the context of high and low cellular glycogen. If glycogen content was low (i.e. 3 mM glucose), oligomycin activated AMPK (Thr-172 phosphorylation; Figure 5D), an effect that was overruled by high cellular glycogen content (i.e. 25 mM glucose). Oligomycin induced activation of AMPK and the consequential Thr-148 phosphorylation further enhanced the interaction of AMPKβ2-WT and R6 (Figure 5D, right panel) under low glycogen

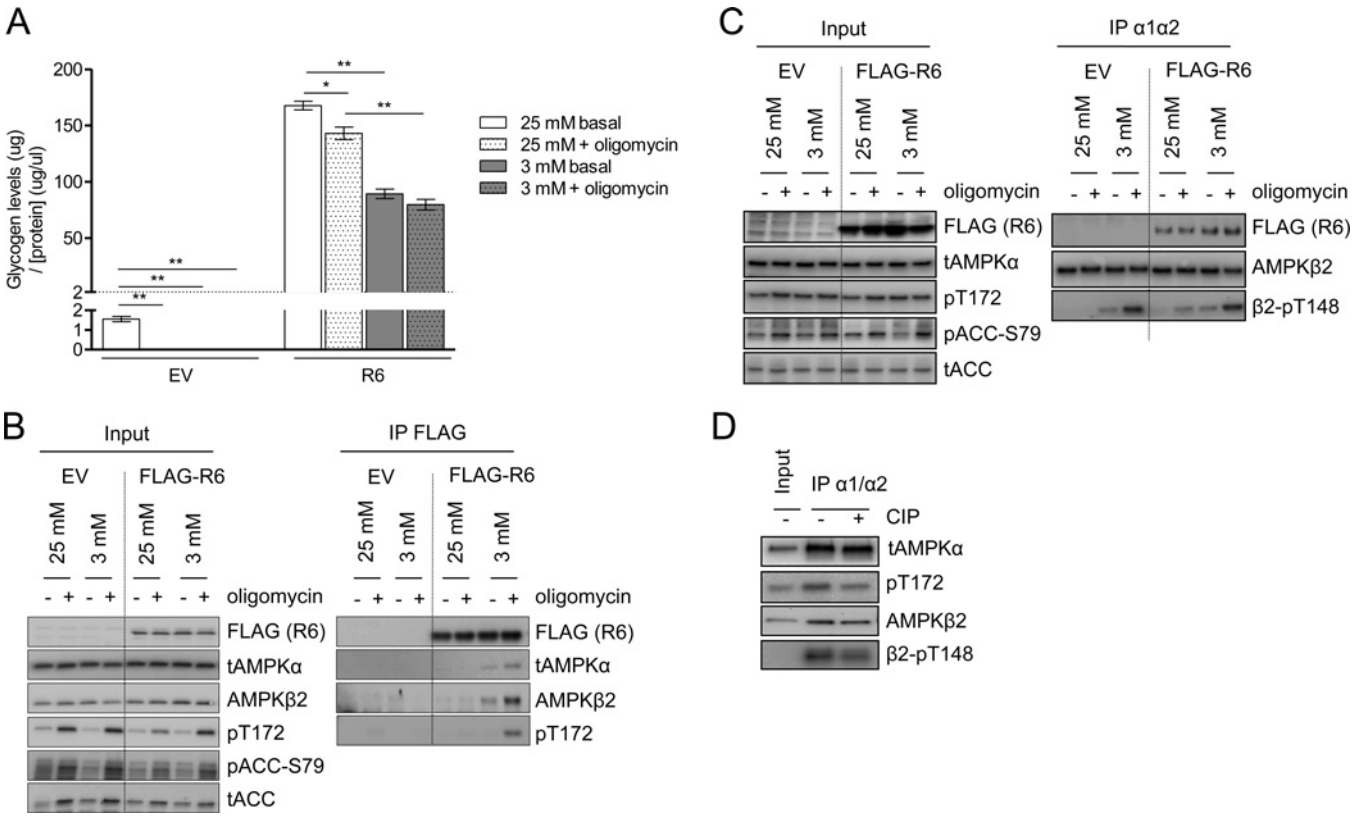

Figure 6 Endogenous AMPKβ2 shows enhanced interaction with R6 upon glycogen depletion in C2C12 myotubes

C2C12 cells stably overexpressing FLAG–R6 were differentiated into myotubes for 4–5 days, and subsequently incubated with high (25 mM) or low (3 mM) glucose for 16 h, followed by 30 min of treatment with oligomycin (5 μM) or DMSO (control). pBabe-puromycin EV was used as control. (**A**) Myocellular glycogen levels were determined using a biochemical glycogen assay, as described in the Materials and methods section. $^{*}P < 0.05$ and $^{**}P < 0.001$; $n = 3$. (**B**) Interaction between AMPKβ2 and R6 was assessed by IP using the anti-FLAG-tag antibody, followed by Western blot analysis using the indicated antibodies. (**C**) Interaction between AMPKβ2 and R6 was assessed by IP using anti-AMPKα1/α2 antibodies, followed by Western blot analysis using the indicated antibodies. (**D**) Mouse gastrocnemius muscle lysate was cleared by centrifugation and subjected to IP using AMPK α1/AMPKα2 antibodies. Immunoprecipitates were maintained on ice either untreated or treated with CIP and then probed by Western blotting using the indicated antibodies. Representative Western blots are shown.

conditions. This interaction was disrupted by high cellular glycogen or by T148D mutation (Figure 5D). These results indicate that glycogen depletion enhances both the AMPKβ2-R6 interaction and phosphorylation of Thr-148. Our data also indicate that phosphorylation of AMPKβ2 at Thr-148 has a different outcome from the AMPKβ2-T148D mutant: whereas the AMPKβ2-T148D mutant is not able to interact with R6, the AMPKβ2-R6 interaction is improved under conditions that enhance AMPKβ2 Thr-148 phosphorylation.

Endogenous AMPKβ2 shows enhanced interaction with R6 upon glycogen depletion in C2C12 myotubes

Furthermore, we explored the significance of cellular glycogen with respect to the AMPKβ2-R6 interaction in C2C12 myotubes, a more physiologically relevant model. Similar to all other tested cell types, endogenous R6 was below detection level in C2C12 cells using a variety of available antibodies (results not shown). Hence, we stably expressed FLAG–R6 or EV control in C2C12 myoblasts. C2C12 cells were then differentiated to myotubes and cultured under high- (i.e. 25 mM) or low- (i.e. 3 mM) glucose concentrations prior to oligomycin treatment. We determined glycogen content and AMPKβ2-R6 interaction for each condition (Figures 6A and 6B). Both lowered glucose availability and oligomycin treatment reduced the myocellular glycogen content below detection level in cells expressing the EV control (Figure 6A). R6 overexpression greatly enhanced the levels of glycogen under basal and treated conditions (Figure 6A). Oligomycin challenged the glycogen levels (Figure 6A) and clearly induced AMPK activation in C2C12 myotubes, under both high- and low-glucose conditions (Figure 6B, left panel). However, as in HEK293T cells, oligomycin-mediated AMPK activation could only be detected in immunoprecipitates from cells that were cultured under low-glycogen conditions (Figure 6B, right panel). As expected, increased interaction of AMPKβ2 with R6 was detected after immunoprecipitating FLAG–R6 from oligomycin-treated cells under low-glycogen conditions (Figure 6B, right panel). By performing the reverse IP using AMPKα1/AMPKα2-directed antibodies, we also detected enhanced FLAG–R6 presence under low-glycogen conditions (Figure 6C). Moreover, we detected Thr-148 phosphorylation of endogenous AMPKβ2, which expectedly was highest in conjunction with low glycogen in oligomycin-treated immunoprecipitates (Figure 6C). We further assessed the presence of Thr-148 phosphorylation in a physiological context. Gastrocnemius muscle was obtained from untreated mice and AMPK was immunoprecipitated from homogenates (Figure 6D). As shown by Western blotting, Thr-148 phosphorylation signal was evident. A decrease in this signal upon incubation with calf intestine phosphatase (CIP) further confirms the phosphorylation event. Therefore, skeletal muscle may operate signalling pathways involving phosphorylated Thr-148. Taken together, in good

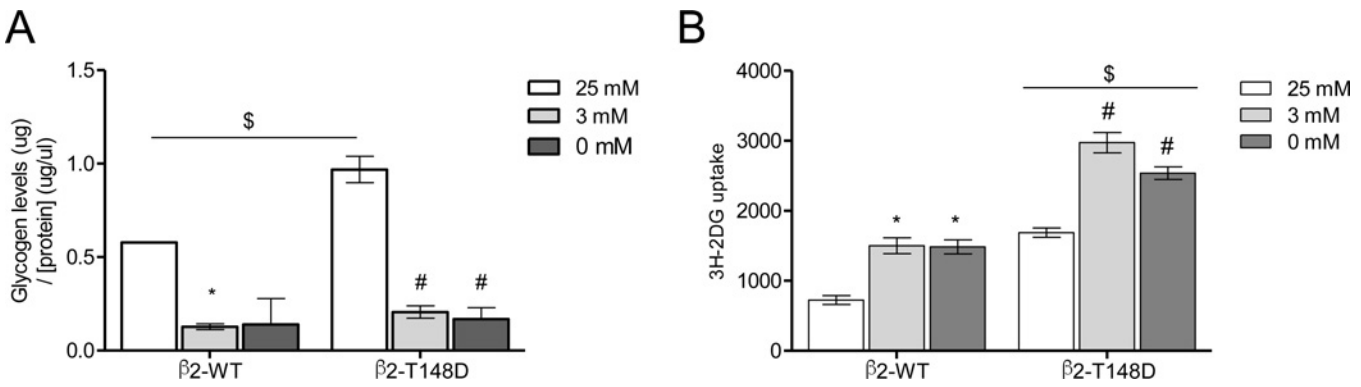

Figure 7 AMPKβ2 Thr-148 mutant enhances glycogen content of C2C12 myotubes

C2C12 cells stably overexpressing AMPKβ2-WT or -T148D mutant were differentiated into myotubes for 4–5 days, and subsequently incubated with high (25 mM), low (3 mM) or no (0 mM) glucose for 16 h. (**A**) Myocellular glycogen levels were determined using a biochemical glycogen assay, as described in the Materials and methods section. $^{*}P < 0.01$ compared with β2-WT with 25 mM glucose, $^{\#}P < 0.05$ compared with β2-T148D with 25 mM glucose, $^{\$}P < 0.05$ β2-WT compared with β2-T148D; $n = 2$. (**B**) Insulin-stimulated glucose uptake was determined as described in the Materials and methods section. $^{*}P < 0.01$ compared with β2-WT with 25 mM glucose, $^{\#}P < 0.01$ compared with β2-T148D with 25 mM glucose, $^{\$}P < 0.01$ β2-WT compared with β2-T148D; $n = 2$.

agreement with our observations in HEK293T cells, the data obtained from C2C12 myotubes support the notion that cellular glycogen content controls AMPKβ2-R6 binding. Also, Thr-148 phosphorylation of endogenous AMPKβ2 occurred in conjunction with R6 interaction in C2C12 myotubes.

AMPKβ2 Thr-148 mutant enhances glycogen content of C2C12 myotubes

We next studied the effect of expressing the AMPKβ2-T148D mutant in C2C12 cells in terms of glucose uptake and glycogen accumulation. To this end, we stably expressed AMPKβ2-WT or -T148D mutant in C2C12 cells, and after differentiation, cells were incubated in the presence of high (25 mM), low (3 mM) or no glucose. Expectedly, the glycogen levels were challenged by low or no glucose incubations (Figure 7A). However, relative to WT, the T148D mutant-overexpressing cells showed significantly higher glycogen content (under high glucose). Since the AMPKβ2-T148D mutant does not associate with glycogen (and R6), these data could indicate a function of the AMPKβ2-T148D mutant that is independent of the glycogen particle, possibly by improving glucose uptake. Indeed, glucose uptake was significantly higher in AMPKβ2-T148D-expressing cells if compared with AMPKβ2-WT under all culturing conditions (Figure 7B).

DISCUSSION

In the present study, we demonstrate the involvement of Thr-148 in the dynamic AMPKβ2-R6 interaction that is governed by glycogen content.

Due to the positioning of Thr-148 in the carbohydrate-binding pocket, the phosphorylation of this residue is incompatible with glycogen binding. Glucose deprivation expectedly resulted in reduced glycogen levels (Figures 4–7). Accordingly, we detected strong AMPKβ2 Thr-148 phosphorylation signals only when glycogen levels were low, which were further augmented by oligomycin treatment (Figure 5). Similar to GS, which dissociates from glycogen in response to glycogen breakdown [32,33], decreased glycogen content may also cause AMPKβ2 and R6 to leave glycogen. In support of such notion, oligomycin-induced AMPK activation augmented AMPKβ2-R6 interaction also in C2C12 myotubes, while further depleting glycogen and inducing Thr-148 phosphorylation (Figure 6), strongly suggesting that these events are linked. In conjunction with lowered glycogen content, oligomycin-induced Thr-172 phosphorylation was also more effective, which ties in with autophosphorylation of Thr-148, i.e. by AMPK. Thus, autophosphorylation of Thr-148 by AMPK may indicate detachment of AMPK from glycogen under conditions that challenge the cellular glycogen level.

We find that phosphorylation of AMPKβ2 at Thr-148 enhanced the binding to R6, whereas AMPKβ2-R6 interaction was completely lost in the AMPKβ2-T148D mutant. The latter results are in agreement with earlier observations, where the AMPKβ1-G147R mutation impaired the ability to interact with R6 [20]. Since AMPKβ Thr-148 is located adjacent to Gly-147, a similar loss of binding to R6 for the Thr-148 mutant was expected. Nevertheless, the molecular mechanism explaining the loss of binding to R6 as a result of T148D mutation remains unclear because Thr-148 phosphorylation was enhanced in conjunction with the AMPKβ2-R6 interaction (Figure 5). In our previous study, we found that the T148D mutant did not bind glycogen [22]. Hence, there are at least two possible explanations: (i) the T148D mutation causes a subtle modification in the conformation of the β2 subunit resulting in the loss of interaction with R6, a process not shared by the physiological phosphorylation of this subunit, or (ii) the interaction of AMPKβ2-WT with R6 that is observed during glycogen degradation evolves from their initial binding at glycogen. These explanations are not mutually exclusive and we formally cannot rule out the former, but there are arguments in support of the latter notion. First, both AMPKβ2 and R6 bind to glycogen via their respective CBM [12,34]. The co-localization of AMPK and R6 to glycogen brings them in close proximity to each other, which may facilitate their subsequent direct interaction, i.e. as a second step during conditions that degrade glycogen. Hence, the possible mechanisms causing AMPKβ2 and R6 to leave the dwindling glycogen particle may include the decreasing surface-binding options. On a diminishing glycogen granule, we can indeed expect the concentration of potential interaction partners to increase dramatically, which may facilitate a direct binding between these proteins concomitant with their detachment from glycogen. This is in accordance with our findings showing that depletion of intracellular glycogen resulted in enhanced AMPKβ2-R6 interaction (Figures 4–6). In particular, the AMPKβ2-R6 complex was more abundant in glucose-deprived or forskolin-treated cells (Figure 4B). Similarly,

in earlier Y2H analyses, low-glucose medium augmented the AMPKβ1-R6 interaction [35]. Secondly, high glycogen content was found to decrease the AMPKβ2-R6 interaction (Figures 4–6), and thus glycogen may in fact rather perturb the direct binding between AMPKβ2 and R6. In addition, AMPKβ2-R6 binding decreased upon treatment of co-IPs with β-CD (Figure 4D). Since the R6-substrate-binding motif partially overlaps with the CBM domain [23], it is conceivable that glycogen competes with R6 binding to AMPK. Thus, our data suggest that low glycogen favours AMPKβ2-R6 interaction, whereas high glycogen content interferes with it. We propose that the AMPKβ2-T148D mutant, due to lack of glycogen-binding affinity, is excluded from the interaction with R6 because this process initiates at glycogen.

AMPK plays an essential role in various biological processes involved in restoring cellular energy homoeostasis. Tuning of such processes requires adequate regulation, and involves AMPK compartmentalization and complex formation with other proteins and substrates. In the present study, we show that R6 preferentially interacts with AMPKβ2, rather than AMPKβ1, pointing to a possible role for this interaction in skeletal muscle. The CBM domain of AMPKβ2 possesses higher binding affinity for carbohydrates such as glycogen than AMPKβ1 [14]. In a more detailed study, the CBM domain of AMPKβ2 bound linear carbohydrates and single α1,6-branched carbohydrates 4–30-fold tighter in comparison with AMPKβ1 [36]. AMPKβ2, as well as R6, are highly expressed in skeletal muscle [3,37], a tissue active in controlling disposal of glucose into glycogen [38]. Thus, it is likely that these proteins contribute to the regulation of myocellular glycogen turnover. *In vivo* studies seemingly contradict the importance of AMPKβ2 in glycogen metabolism: The observed differences in glycogen content were marginal between WT and AMPKβ1/β2-double-knockout mice pre- and post-exercise [39]. In AMPKβ2-knockout mice, muscular glycogen content was reduced pre-exercise and was equal with a slight tendency to increase post-exercise [6,7]. However, since there is a reduction in the levels of skeletal muscle AMPKα1 and AMPKα2 in AMPKβ2-knockout mice and a dramatic reduction of the levels of the AMPK complex subunits in double AMPKβ1/AMPKβ2-knockout mice, it is difficult to make any correlation between the levels of glycogen in these mice and the activity of AMPK. We recently showed that activation of AMPK precedes AMPKβ Thr-148 autophosphorylation to preclude the AMPK complex from binding to glycogen and further data suggested a possible role for Thr-148 phosphorylation in glycogen turnover in several cell lines [22]. Thus, independently of possible functions for AMPK complexes that are bound at glycogen particles, free cytosolic AMPK may also indirectly affect glycogen metabolism, as further supported by T148D overexpression in C2C12 myotubes (Figure 7). Moreover, R6 is a known glycogen-binding protein and PP1-targeting subunit acting as a glycogenic driver [24]. Hence, it is conceivable to expect that the AMPKβ2-R6 interaction is playing an important role in glycogen metabolism in muscle.

In yeast, it was reported earlier that Gal-83 (Snf1 β-subunit orthologue) is involved in binding to Reg1 (PP1 glycogenic subunit orthologue) and studies in mouse pancreatic β-cells revealed that AMPKβ1 interacts with the PP1 glycogen-targeting subunit R6 [20,40]. R6 recruits PP1 to its substrates (e.g. GS and GP) [23], thus playing a critical role in the regulation of glycogen metabolism. Most of the PP1 glycogen-targeting subunits exert their actions through binding to PP1 via a conserved N-terminal PP1-binding motif (RVXF), and interact with PP1 substrates via a conserved C-terminal substrate-binding [WXNXGNYX(L/I)] motif [23]. We have recently shown that R6 utilizes this conserved region to bind to its glycogenic substrates GS and GP [23]. In line with these results, our work indicates that AMPKβ/R6 interaction occurs also via the R6 substrate-binding motif (Figure 2), as a mutation in this domain resulted in loss of interaction, a process that is independent of PP1 binding. However, we did not find evidence for R6/PP1-dependent AMPK dephosphorylation in our study under conditions where the AMPKβ2-R6 interaction was enhanced. This may be attributed to the use of glycogen depletion and mitochondrial poisoning as triggers. Although we find that these treatments are required to induce significant AMPKβ2-R6 interaction, their application necessarily goes along with elevated AMP levels and consequent protection from Thr-172 dephosphorylation [41]. In MIN6 pancreatic β-cells, the PP1-R6 complex was responsible for AMPK dephosphorylation at Thr-172 in response to high extracellular glucose [20]. In HEK293T cells, we find that glucose re-availability leads to a transient decrease in Thr-172 phosphorylation (Figure 4C). In the same experiment, AMPKβ2-R6 interaction disappeared time-dependently after recovery with high glucose. Hence, the idea that R6 could act as a scaffold to bring AMPKβ2 in close proximity to the PP1 phosphatase warrants further investigation. The present data establish that AMPKβ2-R6 complex formation and dissociation are reversible and dynamic processes that involve the substrate-binding site of R6. Taken together, we shed new light on the molecular events that govern the interaction of AMPK with R6.

AUTHOR CONTRIBUTION

Yvonne Oligschlaeger, Marie Miglianico, Vivian Dahlmans, Carla Rubio-Villena, Dipanjan Chanda, Maria Adelaida Garcia-Gimeno, Will Coumans, Yilin Liu, Pascual Sanz and Dietbert Neumann designed and carried out the experiments. Yvonne Oligschlaeger, Pascual Sanz and Dietbert Neumann wrote the manuscript. Willem Voncken, Joost Luiken and Jan Glatz contributed with material, provided conceptual input and assisted in the manuscript preparation. All authors reviewed the results and approved the final version of the manuscript.

ACKNOWLEDGEMENTS

We thank the members of the Molecular Genetics department of Maastricht University for helpful comments and support.

FUNDING

This work was supported by the VIDI-Innovational Research Grant from the Netherlands Organization for Scientific Research (NWO-ALW) [grant number 864.10.007 (to D.N.)]; the Spanish Ministry of Education and Science [grant number SAF2014-54604-C3-1-R (to P.S.)]; and the Generalitat Valenciana [grant number PrometeoII/2014/029 (to P.S.)]. D.C. is the recipient of a Marie Curie fellowship [grant number PIIF-GA-2012-332230].

REFERENCES

1 Jornayvaz, F.R., Samuel, V.T. and Shulman, G.I. (2010) The role of muscle insulin resistance in the pathogenesis of atherogenic dyslipidemia and nonalcoholic fatty liver disease associated with the metabolic syndrome. Annu. Rev. Nutr. **30**, 273–290 CrossRef PubMed

2 Kurth-Kraczek, E.J., Hirshman, M.F., Goodyear, L.J. and Winder, W.W. (1999) 5′ AMP-activated protein kinase activation causes GLUT4 translocation in skeletal muscle. Diabetes **48**, 1667–1671 CrossRef PubMed

3 Thornton, C., Snowden, M.A. and Carling, D. (1998) Identification of a novel AMP-activated protein kinase beta subunit isoform that is highly expressed in skeletal muscle. J. Biol. Chem. **273**, 12443–12450 CrossRef PubMed

4 Chen, Z., Heierhorst, J., Mann, R.J., Mitchelhill, K.I., Michell, B.J., Witters, L.A., Lynch, G.S., Kemp, B.E. and Stapleton, D. (1999) Expression of the AMP-activated protein kinase beta1 and beta2 subunits in skeletal muscle. FEBS Lett. **460**, 343–348 CrossRef PubMed

5 Dzamko, N., van Denderen, B.J., Hevener, A.L., Jorgensen, S.B., Honeyman, J., Galic, S., Chen, Z.P., Watt, M.J., Campbell, D.J., Steinberg, G.R. and Kemp, B.E. (2010) AMPK beta1 deletion reduces appetite, preventing obesity and hepatic insulin resistance. J. Biol. Chem. **285**, 115–122 CrossRef PubMed

6 Dasgupta, B., Ju, J.S., Sasaki, Y., Liu, X., Jung, S.R., Higashida, K., Lindquist, D. and Milbrandt, J. (2012) The AMPK beta2 subunit is required for energy homeostasis during metabolic stress. Mol. Cell. Biol. **32**, 2837–2848 CrossRef PubMed

7 Steinberg, G.R., O'Neill, H.M., Dzamko, N.L., Galic, S., Naim, T., Koopman, R., Jørgensen, S.B., Honeyman, J., Hewitt, K., Chen, Z.P. et al. (2010) Whole body deletion of AMP-activated protein kinase {beta}2 reduces muscle AMPK activity and exercise capacity. J. Biol. Chem. **285**, 37198–37209 CrossRef PubMed

8 McGee, S.L., Howlett, K.F., Starkie, R.L., Cameron-Smith, D., Kemp, B.E. and Hargreaves, M. (2003) Exercise increases nuclear AMPK alpha2 in human skeletal muscle. Diabetes **52**, 926–928 CrossRef PubMed

9 Kodiha, M., Rassi, J.G., Brown, C.M. and Stochaj, U. (2007) Localization of AMP kinase is regulated by stress, cell density, and signaling through the MEK→ERK1/2 pathway. Am. J. Physiol. Cell Physiol. **293**, C1427–C1436 CrossRef PubMed

10 Carling, D., Clarke, P.R., Zammit, V.A. and Hardie, D.G. (1989) Purification and characterization of the AMP-activated protein kinase. Copurification of acetyl-CoA carboxylase kinase and 3-hydroxy-3-methylglutaryl-CoA reductase kinase activities. Eur. J. Biochem. **186**, 129–136 CrossRef PubMed

11 Kazgan, N., Williams, T., Forsberg, L.J. and Brenman, J.E. (2010) Identification of a nuclear export signal in the catalytic subunit of AMP-activated protein kinase. Mol. Biol. Cell **21**, 3433–3442 CrossRef PubMed

12 Polekhina, G., Gupta, A., Michell, B.J., van Denderen, B., Murthy, S., Feil, S.C., Jennings, I.G., Campbell, D.J., Witters, L.A., Parker, M.W. et al. (2003) AMPK β subunit targets metabolic stress sensing to glycogen. Curr. Biol. **13**, 867–871 CrossRef PubMed

13 Hudson, E.R., Pan, D.A., James, J., Lucocq, J.M., Hawley, S.A., Green, K.A., Baba, O., Terashima, T. and Hardie, D.G. (2003) A novel domain in AMP-activated protein kinase causes glycogen storage bodies similar to those seen in hereditary cardiac arrhythmias. Curr. Biol. **13**, 861–866 CrossRef PubMed

14 Koay, A., Woodcroft, B., Petrie, E.J., Yue, H., Emanuelle, S., Bieri, M., Bailey, M.F., Hargreaves, M., Park, J.T., Park, K.H. et al. (2010) AMPK beta subunits display isoform specific affinities for carbohydrates. FEBS Lett. **584**, 3499–3503 CrossRef PubMed

15 Wojtaszewski, J.F., Jorgensen, S.B., Hellsten, Y., Hardie, D.G. and Richter, E.A. (2002) Glycogen-dependent effects of 5-aminoimidazole-4-carboxamide (AICA)-riboside on AMP-activated protein kinase and glycogen synthase activities in rat skeletal muscle. Diabetes **51**, 284–292 CrossRef PubMed

16 Hunter, R.W., Treebak, J.T., Wojtaszewski, J.F. and Sakamoto, K. (2011) Molecular mechanism by which AMP-activated protein kinase activation promotes glycogen accumulation in muscle. Diabetes **60**, 766–774 CrossRef PubMed

17 Fong, N.M., Jensen, T.C., Shah, A.S., Parekh, N.N., Saltiel, A.R. and Brady, M.J. (2000) Identification of binding sites on protein targeting to glycogen for enzymes of glycogen metabolism. J. Biol. Chem. **275**, 35034–35039 CrossRef PubMed

18 Heroes, E., Lesage, B., Gornemann, J., Beullens, M., Van Meervelt, L. and Bollen, M. (2013) The PP1 binding code, a molecular-lego strategy that governs specificity. FEBS J. **280**, 584–595 CrossRef PubMed

19 Armstrong, C.G., Browne, G.J., Cohen, P. and Cohen, P.T.W. (1997) PPP1R6, a novel member of the family of glycogen-targetting subunits of protein phosphatase 1. FEBS Lett. **418**, 210–214 CrossRef PubMed

20 Garcia-Haro, L., Garcia-Gimeno, M.A., Neumann, D., Beullens, M., Bollen, M. and Sanz, P. (2010) The PP1-R6 protein phosphatase holoenzyme is involved in the glucose-induced dephosphorylation and inactivation of AMP-activated protein kinase, a key regulator of insulin secretion, in MIN6 beta cells. FASEB J. **24**, 5080–5091 CrossRef PubMed

21 Sanz, P., Alms, G.R., Haystead, T.A. and Carlson, M. (2000) Regulatory interactions between the Reg1-Glc7 protein phosphatase and the Snf1 protein kinase. Mol. Cell. Biol. **20**, 1321–1328 CrossRef PubMed

22 Oligschlaeger, Y., Miglianico, M., Chanda, D., Scholz, R., Thali, R.F., Tuerk, R., Stapleton, D.I., Gooley, P.R. and Neumann, D. (2015) The recruitment of AMP-activated protein kinase to glycogen is regulated by autophosphorylation. J. Biol. Chem. **290**, 11715–11728 CrossRef PubMed

23 Rubio-Villena, C., Sanz, P. and Garcia-Gimeno, M.A. (2015) Structure–function analysis of PPP1R3D, a protein phosphatase 1 targeting subunit, reveals a binding motif for 14-3-3 proteins which regulates its glycogenic properties. PLoS One **10**, e0131476 CrossRef PubMed

24 Rubio-Villena, C., Garcia-Gimeno, M.A. and Sanz, P. (2013) Glycogenic activity of R6, a protein phosphatase 1 regulatory subunit, is modulated by the laforin–malin complex. Int. J. Biochem. Cell Biol. **45**, 1479–1488 CrossRef PubMed

25 Gimeno-Alcaniz, J.V. and Sanz, P. (2003) Glucose and type 2A protein phosphatase regulate the interaction between catalytic and regulatory subunits of AMP-activated protein kinase. J. Mol. Biol. **333**, 201–209 CrossRef PubMed

26 Kinsella, T.M. and Nolan, G.P. (1996) Episomal vectors rapidly and stably produce high-titer recombinant retrovirus. Hum. Gene Ther. **7**, 1405–1413 CrossRef PubMed

27 Morgenstern, J.P. and Land, H. (1990) Advanced mammalian gene transfer: high titre retroviral vectors with multiple drug selection markers and a complementary helper-free packaging cell line. Nucleic Acids Res. **18**, 3587–3596 CrossRef PubMed

28 Voncken, J.W., Niessen, H., Neufeld, B., Rennefahrt, U., Dahlmans, V., Kubben, N., Holzer, B., Ludwig, S. and Rapp, U.R. (2005) MAPKAP kinase 3pK phosphorylates and regulates chromatin association of the polycomb group protein Bmi1. J. Biol. Chem. **280**, 5178–51787 CrossRef PubMed

29 Schwenk, R.W., Dirkx, E., Coumans, W.A., Bonen, A., Klip, A., Glatz, J.F. and Luiken, J.J. (2010) Requirement for distinct vesicle-associated membrane proteins in insulin- and AMP-activated protein kinase (AMPK)-induced translocation of GLUT4 and CD36 in cultured cardiomyocytes. Diabetologia **53**, 2209–2219 CrossRef PubMed

30 Skehel, J.M. (2004) Preparation of extracts from animal tissues. Methods Mol. Biol. **244**, 15–20 PubMed

31 Singh, P.K., Singh, S. and Ganesh, S. (2012) The laforin–malin complex negatively regulates glycogen synthesis by modulating cellular glucose uptake via glucose transporters. Mol. Cell. Biol. **32**, 652–663 CrossRef PubMed

32 Nielsen, J.N., Derave, W., Kristiansen, S., Ralston, E., Ploug, T. and Richter, E.A. (2001) Glycogen synthase localization and activity in rat skeletal muscle is strongly dependent on glycogen content. J. Physiol. **531**, 757–769 CrossRef PubMed

33 Prats, C., Cadefau, J.A., Cusso, R., Qvortrup, K., Nielsen, J.N., Wojtaszewski, J.F., Hardie, D.G., Stewart, G., Hansen, B.F. and Ploug, T. (2005) Phosphorylation-dependent translocation of glycogen synthase to a novel structure during glycogen resynthesis. J. Biol. Chem. **280**, 23165–23172 CrossRef PubMed

34 Machovic, M. and Janecek, S. (2006) Starch-binding domains in the post-genome era. Cell. Mol. Life Sci. **63**, 2710–2724 CrossRef PubMed

35 Garcia-Haro, L., Garcia-Gimeno, M.A., Neumann, D., Beullens, M., Bollen, M. and Sanz, P. (2012) Glucose-dependent regulation of AMP-activated protein kinase in MIN6 beta cells is not affected by the protein kinase A pathway. FEBS Lett. **586**, 4241–4247 CrossRef PubMed

36 Mobbs, J.I., Koay, A., Di Paolo, A., Bieri, M., Petrie, E.J., Gorman, M.A., Doughty, L., Parker, M.W., Stapleton, D.I., Griffin, M.D. and Gooley, P.R. (2015) Determinants of oligosaccharide specificity of the carbohydrate-binding modules of AMP-activated protein kinase. Biochem. J. **468**, 245–257 CrossRef PubMed

37 Montori-Grau, M., Guitart, M., Garcia-Martinez, C., Orozco, A. and Gomez-Foix, A.M. (2011) Differential pattern of glycogen accumulation after protein phosphatase 1 glycogen-targeting subunit PPP1R6 overexpression, compared to PPP1R3C and PPP1R3A, in skeletal muscle cells. BMC Biochem. **12**, 57 CrossRef PubMed

38 Ren, J.M., Marshall, B.A., Gulve, E.A., Gao, J., Johnson, D.W., Holloszy, J.O. and Mueckler, M. (1993) Evidence from transgenic mice that glucose transport is rate-limiting for glycogen deposition and glycolysis in skeletal muscle. J. Biol. Chem. **268**, 16113–16115 PubMed

39 O'Neill, H.M., Maarbjerg, S.J., Crane, J.D., Jeppesen, J., Jorgensen, S.B., Schertzer, J.D., Shyroka, O., Kiens, B., van Denderen, B.J., Tarnopolsky, M.A. et al. (2011) AMP-activated protein kinase (AMPK) beta1beta2 muscle null mice reveal an essential role for AMPK in maintaining mitochondrial content and glucose uptake during exercise. Proc. Natl. Acad. Sci. U.S.A. **108**, 16092–16097 CrossRef PubMed

40 Mangat, S., Chandrashekarappa, D., McCartney, R.R., Elbing, K. and Schmidt, M.C. (2010) Differential roles of the glycogen-binding domains of beta subunits in regulation of the Snf1 kinase complex. Eukaryot. Cell **9**, 173–183 CrossRef PubMed

41 Suter, M., Riek, U., Tuerk, R., Schlattner, U., Wallimann, T. and Neumann, D. (2006) Dissecting the role of 5′-AMP for allosteric stimulation, activation, and deactivation of AMP-activated protein kinase. J. Biol. Chem. **281**, 32207–32216 CrossRef PubMed

Received 30 September 2015/22 January 2016; accepted 1 February 2016
Accepted Manuscript online 1 February 2016, doi:10.1042/BJ20151035